



ChemComm

**Four-electron Oxidation and One-electron Reduction of the
Bis(terphenylthiolate) U(II) Complex, U(SAriPr6)2 [AriPr6
= C6H3-2,6-(C6H2-2,4,6-iPr3)2]**

Journal:	<i>ChemComm</i>
Manuscript ID	CC-COM-04-2025-002284.R1
Article Type:	Communication

SCHOLARONE™
Manuscripts

Four-electron Oxidation and One-electron Reduction of the Bis(terphenylthiolate) U(II) Complex, $U(SAr^{iPr6})_2$ [$Ar^{iPr6} = C_6H_3-2,6-(C_6H_2-2,4,6-iPr_3)_2$]

Received 00th January 20xx,
Accepted 00th January 20xx

DOI: 10.1039/x0xx00000x

Joshua D. Queen, Eric Ma, Ahmadreza Rajabi, Joseph W. Ziller, Philipp Furche* and William J. Evans*

The utility of the sterically bulky terphenylthiolate ligand, $(SAr^{iPr6})^{1-}$ in expanding uranium redox chemistry has been explored. Reduction of $U(SAr^{iPr6})_2$ forms the U(II) complex, $U(SAr^{iPr6})_2$, in which the metal is protected by the flanking arene rings of the ligand, but they move out of the way to accommodate the four electron reduction of $PhN=NPh$ to form the U(VI) bis(imido) product $U(SAr^{iPr6})_2(=NPh)_2(THF)_2$. The KC_8 reduction of $U(SAr^{iPr6})_2$ generates a more reduced complex, $KU(\mu-SAr^{iPr6})_2$, initially identified by a -2.55 V vs Fc^+/Fc electrochemical reduction event in THF.

The reductive redox chemistry of uranium is receiving increasing amounts of attention following the isolation of numerous examples of U(II) complexes¹⁻⁸ and their reduction products identified as U(I) synthons.⁸⁻¹⁰ In addition, a U(I) metallocene anion, $[(C_5^iPr_5)_2U]^{1-}$, has been reported.¹¹ As shown in Figure 1, all of these “U(I)” examples have involved ligands with first row main group donor atoms, C, N, or O. In efforts to extend the coordination chemistry of low oxidation state actinides to second row donor atoms, we have examined the chemistry of uranium with the sterically bulky terphenylthiolate ligand, $[S[C_6H_3-2,6-(C_6H_2-2,4,6-iPr_3)_2]]^{1-}$, $(SAr^{iPr6})^{1-}$.

The $(SAr^{iPr6})^{1-}$ ligand and related $(OAr^{iPr6})^{1-}$ and $(NHAr^{iPr6})^{1-}$ ligands were extensively studied since the 1990s by Power, et al.¹²⁻¹⁴ with transition metals¹⁵⁻²¹ and main group elements^{22, 23} to stabilize low oxidation state, low coordinate complexes. Niemeyer, et al. demonstrated in the early 2000s that the $(SAr^{iPr6})^{1-}$ ligand stabilizes unsolvated f-block complexes $Ln(SAr^{iPr6})_2$ for Sm(II), Eu(II), and Yb(II)^{24,25} that have η^6 -interactions with the flanking aryl rings. The rare-earth complexes $Sm(OAr^{iPr6})_2$ ²⁶ and $Ln[N(H)Ar^{iPr6}]_2$ ($Ln = Sc, Y, La, Sm, Eu, Tm, \text{ and } Yb$)^{27, 28} have similar structures. We recently employed the $(SAr^{iPr6})^{1-}$ ligand to isolate the first examples of Ln(II) complexes of La, Nd, and Tm²⁹ with second row main group donor atoms and now extend this chemistry to uranium

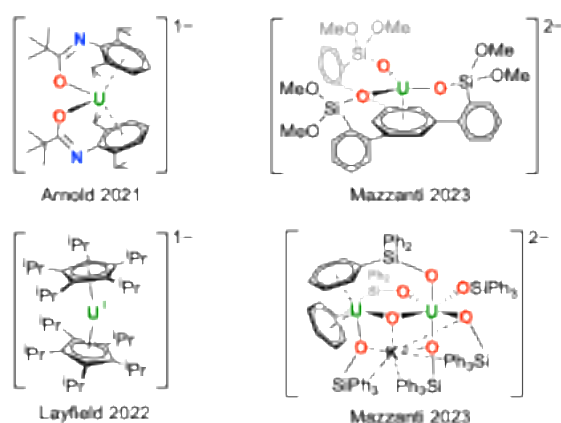
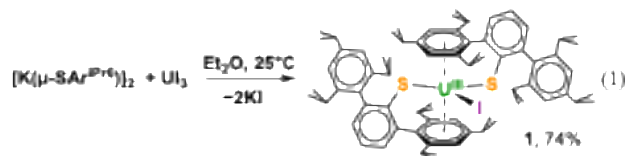


Figure 1. Examples of molecular complexes of uranium(I) and uranium(II) synthons with reduced arene ligands.

since the only U(II) complex with this type of ligand was $U[N(H)Ar^{iPr6}]_2$.⁴ While this work was in progress, U(IV) and U(III) complexes of $(SAr^{iPr6})^{1-}$ were published.³⁰

The reaction of $[K(\mu-SAr^{iPr6})_2]^{12}$ with UCl_3 ³¹ in Et_2O affords the purple uranium(III) complex $U(SAr^{iPr6})_2$, **1**, in 74% yield, eq 1. Analogous reactions by Goodwin, et al. with chloride and



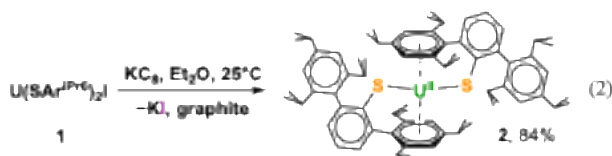
borohydride starting materials were shown to be more complicated although $U(SAr^{iPr6})_2(BH_4)$ was readily prepared.³⁰ The X-ray crystal structure of **1**, Figure S1, shows the uranium atom sandwiched by two η^6 -arene rings with the iodide and two sulfur donor atoms in between in a trigonal arrangement. The

COMMUNICATION

ChemComm

complexes $\text{Ln}(\text{EAr}^{\text{iPr}_6})_2\text{X}$ ($\text{E} = \text{N}(\text{H}), \text{S}, \text{Se}$; $\text{X} = \text{Cl}, \text{I}$),^{24, 27-29, 32} $\text{U}[\text{N}(\text{H})\text{Ar}^{\text{iPr}_6}]_2$,⁴ and $\text{U}(\text{SAr}^{\text{iPr}_6})_2(\text{BH}_4)$ ³⁰ share this structural motif. Metrical parameters are discussed in the SI.

Stoichiometric reduction of purple **1** with KC_8 in Et_2O , eq 2, generated the dark green neutral uranium(II) thiolate, $\text{U}(\text{SAr}^{\text{iPr}_6})_2$, **2**, in 84% yield. Slow evaporation of an *n*-hexane solution of the highly soluble **2** provided green-brown needles suitable for X-ray crystallography.



The structure of **2**, Figure 1, contains 2.763(4) and 2.772(4) Å U–S bond lengths similar to the 2.7590(5) and 2.8226(5) Å U–S bonds in **1** and there is a widening of the S–U–S angle from the 126.06(2)° in **1** to 132.5(1)° in **2**. The Cnt–U–Cnt angle is 152.0(4)°. In comparison, the N–U–N and Cnt–U–Cnt angles in $\text{U}[\text{N}(\text{H})\text{Ar}^{\text{iPr}_6}]_2$ are 99.2(1)° and 130.26(2)°, respectively. These differences could be due to the longer U–S bonds (cf. the 2.330(2) Å U–N bonds in $\text{U}[\text{N}(\text{H})\text{Ar}^{\text{iPr}_6}]_2$) and the greater flexibility of the $\text{C}_{\text{ipso}}\text{--S--U}$ angles, 112.7(3)° and 113.8(3)° in **2**, vs the 130.2(2)° $\text{C}_{\text{ipso}}\text{--N--U}$ angles in $\text{U}[\text{N}(\text{H})\text{Ar}^{\text{iPr}_6}]_2$ that are constrained by the hydrogen substituent on the nitrogen donor.

The U–Cnt distances in **2** are quite different, 2.35(2) and 2.52(2) Å, from the 2.573(3) and 2.583(3) Å distances in $\text{U}[\text{N}(\text{H})\text{Ar}^{\text{iPr}_6}]_2$.⁴ The closer ring has a boat-like distortion from planarity with a fold angle of 19°. The C–C bond distances in the two η^6 -arene rings range between 1.39(2)–1.46(2) Å, but the large error limits preclude further analysis.

The electronic spectrum of **1** features an absorbance maximum at 475 nm while that of **2** shows only a broad absorbance across the visible spectrum that sharply increases starting at ca. 500 nm (See SI). These are similar to the amide analogs.⁴ The Evans method 298 K solution magnetic moment of **2** was found to be 2.7–2.8 μ_{B} , which can be compared with the 2.3–2.4 μ_{B} moments reported for $5f^4$ U(II) compounds^{2, 4, 8}

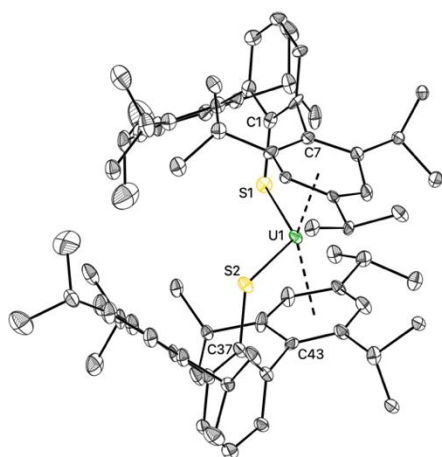


Figure 2. Molecular structure of **2** with ellipsoids drawn at 30% probability. Hydrogen atoms not shown for clarity.

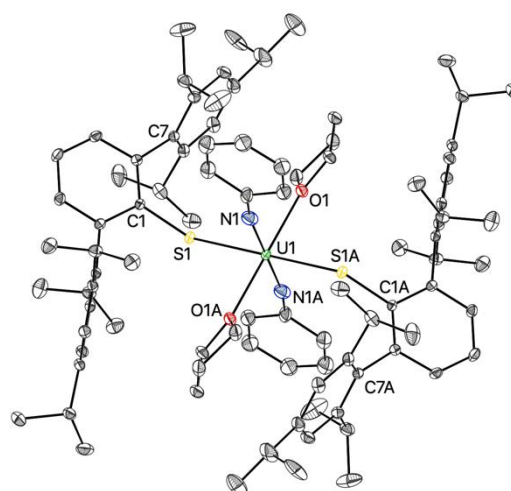
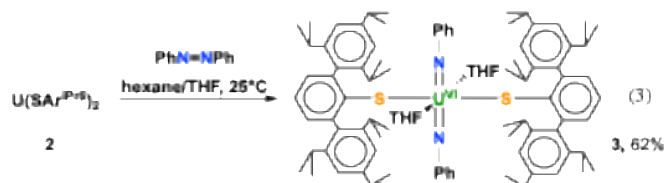


Figure 3. Molecular structure of **3** with ellipsoids drawn at 30% probability. Hydrogen atoms are not shown for clarity.

and the 2.26 μ_{B} moment reported for $5f^36d^1$ $\{[(\text{C}_5\text{H}_2(\text{SiMe}_3)_2)_3\text{U}^{\text{II}}]^{1-}\}$.³

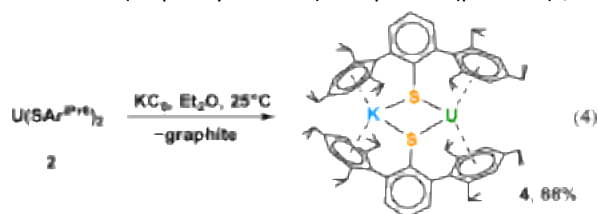
The ability of **2** to participate in multielectron reduction chemistry was demonstrated by its reaction with azobenzene, eq 3. This reaction yielded brown crystals of the U(VI) *trans*-bis(imido) product $\text{U}(\text{SAr}^{\text{iPr}_6})_2(=\text{NPh})_2(\text{THF})_2$, **3**, in a reaction which is a formal U(II) to U(VI) four-electron transformation. The four-electron reduction of $\text{PhN}=\text{NPh}$ at a single metal was first observed for a $5d^4$ W(II) η^6 -arene complex³³ and was recently extended to *f*-element chemistry by the reaction of $\{[(\text{Me}_3\text{Si})_2\text{N}]_3\text{U}^{\text{II}}\}^{1-}$ and “masked U(II)” species with azobenzene.³⁴⁻³⁶



The structure of **3**, Figure 2, is inversion symmetric with an approximately octahedral geometry around the U atom. The short 1.928(3) Å U=N bonds are typical of U(VI) bis(imido) compounds³⁷⁻⁴¹ and the 2.7081(6) Å U–S bonds are close to the 2.7297(7) Å U–S distances in $\text{U}(\text{SPh})_2(=\text{N}^t\text{Bu})_2(\text{py})_2$.³⁹ Notably, the flanking η^6 -arene ligands have completely disassociated from the U atom, demonstrating that the steric bulk protecting the U(II) center in **2** can readily move out of the way to accommodate reactivity.

The cyclic voltammogram of **2**, Figure S2, revealed a prominent reduction event in THF at -2.55 V vs $\text{Fc}^{+/0}$. This is surprisingly similar to several U(III)/U(II) reduction potentials in the literature: $\text{U}\{[\text{OSi}(\text{OMe})_2\text{C}_6\text{H}_4]_3\text{C}_6\text{H}_3\}$,⁸ -2.45 V; $\text{U}\{[\text{Ad},\text{MeArO}]_3\text{mes}\}$, -2.50 V;² $(\text{C}_5^i\text{Pr}_5)_2\text{U}$, -2.33 V;⁴² $(\text{C}_5\text{H}_4\text{SiMe}_3)_3\text{U}$, -2.26 V;⁴³ $[\text{C}_5\text{H}_3(\text{SiMe}_3)_2]_3\text{U}$, -2.73 V.⁴³ In comparison the $[(\text{C}_5^i\text{Pr}_5)_2\text{U}]^{0/1-}$ potential was reported to be -2.85 V.¹¹ and the U(II)/“U(I)” redox couple for $\text{U}\{[\text{OSi}(\text{OMe})_2\text{C}_6\text{H}_4]_3\text{C}_6\text{H}_3\}$ is -3.27 V vs $\text{Fc}^{+/0}$.⁸ The CV of **2** was very promising for accessing a “U(I)” compound and the chemical reduction of **2** was investigated. Treating **2** with KC_8 in

Et_2O , eq 4, gave a rapid green to brown color change. Black crystals were grown from the supernatant and identified as the bimetallic bis(terphenylthiolate) complex $\text{KU}(\mu\text{-SAr}^{\text{iPr}_6})_2$, **4**.



The structure of **4**, Figure 3, is strikingly similar to the group 1 thiolate dimers $\{\text{M}(\mu\text{-SAr}^{\text{iPr}_6})\}_2$ ($\text{M} = \text{Li-Cs}$)¹² in which the metal atoms of the $\text{M}_2(\mu\text{-S})_2$ core are complexed by flanking aryl rings from each terphenyl ligand. The S–U–S angle has narrowed substantially to $62.78(6)^\circ$ from 132.5° in **2**. The $2.887(2)$ and $2.902(2)$ Å U–S distances in **4** are *ca.* 0.1–0.2 Å longer than those in **1**, **2**, **3**, and the related U(IV) and U(III) $(\text{SAr}^{\text{iPr}_6})_2$ compounds³⁰ as expected for bridging ligands.

The K and U in **4** are structurally distinguished by the nature of their coordinated terphenyl flanking arenes. The rings near K in **4** retain their planarity with long $3.13(1)$ and $3.15(1)$ Å K–C_{nt} distances, while those oriented toward U have shorter U–C_{nt} distances of $2.32(1)$ and $2.42(1)$ Å and have undergone boat-like distortions with fold angles of $22.7(7)^\circ$ and $7.4(7)^\circ$, respectively. This distortion is consistent with δ -back-bonding from the U orbitals to the arene π^* orbitals and partial reduction of the arene ring.^{9, 28, 29, 44, 45} As in **2**, the error limits on the $1.39(1)$ to $1.45(1)$ C–C bond distances in the rings are too large to provide statistically meaningful comparisons.

The stepwise reduction of **1** to **2** and then **4** with KC_8 is in marked contrast to the synthesis of $\text{U}[\text{N}(\text{H})\text{Ar}^{\text{iPr}_6}]_2$ which was prepared in high yield from $\text{U}[\text{N}(\text{H})\text{Ar}^{\text{iPr}_6}]_2$ using an excess of KC_8 .⁴ This difference could be due to increased flexibility of the C–S–U linkages compared to C–N(H)–U which allows for each metal to be complexed by two arene groups and bridging thiolate groups. Differences in the structures of the potassium thiolate and amide salts are in support of this. While $[\text{K}(\mu\text{-SAr}^{\text{iPr}_6})]_2$ has a dimeric structure,¹² the potassium amide crystallizes as the monomer $[\text{K}(\text{Et}_2\text{O})_2(\text{NHAr}^{\text{iPr}_6})]$.⁴⁶

The UV-visible spectrum of **4** showed only an absorbance at 280 that tails into the visible with a shoulder feature at *ca.* 400

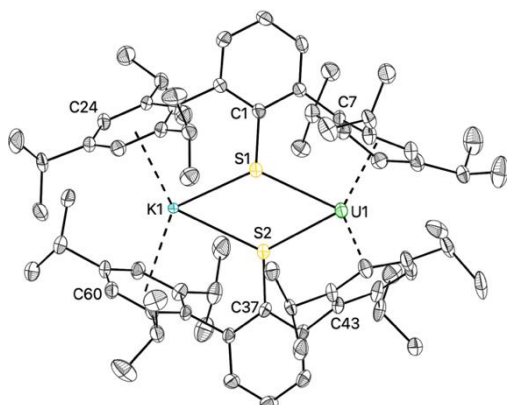


Figure 4. Molecular structure of **4** with ellipsoids drawn at 30%. Hydrogen atoms are not shown for clarity.

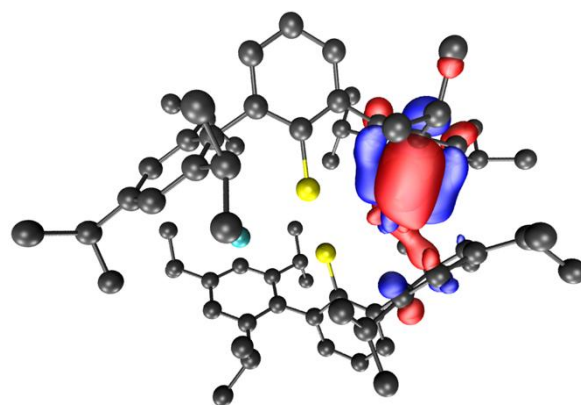


Figure 5. Highest occupied molecular orbital in **4** drawn with a contour value of 0.03.

nm. No resonances attributable to **4** were observed in the ^1H NMR spectrum in benzene and the 298 K Evans method magnetic moment was found to be 2.3–2.4 μ_B . This is similar to the 2.20–2.46 μ_B moments reported for the formally “U(I)” species with reduced arene ligands,^{8–10} whereas $[(\text{C}_5\text{iPr}_5)_2\text{U}]^-$ has a 5.35 μ_B moment at 300 K and was assigned a $5f^36d^1(7s/6d)^1$ ground state.¹¹

Electronic structure calculations using density functional theory (DFT) provided optimized structures that matched the X-ray data for **2** and **4** (see SI for details). Calculations on **2** indicated that the disparate U–C_{nt} distances and UV-visible spectrum were consistent with a quintet ground state. Natural population analysis (NPA) of the spin density indicated unpaired electron populations of 2.83 in U f orbitals, 0.39 in U d orbitals, and 0.35 in the proximal arene ring. Quartet and sextet ground states for **4** were found to be within 5 kcal mol^{−1} with the quartet being lowest and providing the best match to the X-ray and UV-visible data. The quartet ground state features three electrons in U 5f orbitals that interact with the arene rings, and a doubly-occupied δ -bonding combination, Figure 5, derived from two 6d orbitals with strong overlap with arene π^* orbitals in the proximal ring. As recently pointed out in a review of uranium arene interactions,⁴⁵ more extensive physical measurements will be needed in the future to establish the detailed nature of the uranium arene interactions in **4**.

In conclusion, we have shown that the hexa-isopropyl-terphenylthiolate ligand allows the isolation of a neutral uranium(II) thiolate complex which can effect four electron reduction chemistry. Complex **2** is readily reduced further by one electron to the bimetallic thiolate complex $\text{KU}(\mu\text{-SAr}^{\text{iPr}_6})_2$, **4**. Complex **4** has significant interactions between U and the π^* orbitals of the coordinated arene rings which are distorted from planarity that complicate the definitive identification of formal oxidation state. Further investigations into the electronic description of this complex and its utility in multi-electron reactivity are underway.

We thank the Heavy Element Chemistry Program of the Chemical Sciences, Geosciences, and Biosciences Division of the Office of Basic Energy Sciences of the U.S. Department of Energy for support of the experimental parts of this study through DE-SC0004739 (to WJE). Theoretical studies were supported by the National Science Foundation under CHE-2102568 (to FF). A.R. thanks the Eddleman Quantum Institute for support. We thank

the UC Irvine Materials Research Institute (IMRI), supported in part by the National Science Foundation through the UC Irvine Materials Research Science and Engineering Center (DMR-2011967), for use of the facilities

Data availability

CCDC numbers 2413501 (1), 2413502 (2), 2413599 (3), and 2416631 (4) contain the crystallographic data associated with this paper. Experimental details, computational details, and spectroscopy data are reported in the supporting information.

Conflicts of interest

Principal Investigator Filipp Furche has an equity interest in TURBOMOLE GmbH. The terms of this arrangement have been reviewed and approved by the University of California, Irvine, in accordance with its conflict of interest policies.

Notes and references

- M. R. MacDonald, M. E. Fieser, J. E. Bates, J. W. Ziller, F. Furche and W. J. Evans, *J. Am. Chem. Soc.*, 2013, **135**, 13310-13313.
- H. S. La Pierre, A. Scheurer, F. W. Heinemann, W. Hieringer and K. Meyer, *Angew. Chem., Int. Ed.*, 2014, **53**, 7158-7162.
- C. J. Windorff, M. R. MacDonald, K. R. Meihaus, J. W. Ziller, J. R. Long and W. J. Evans, *Chem. Eur. J.*, 2016, **22**, 772-782.
- B. S. Billow, B. N. Livesay, C. C. Mokhtarzadeh, J. McCracken, M. P. Shores, J. M. Boncella and A. L. Odom, *J. Am. Chem. Soc.*, 2018, **140**, 17369-17373.
- A. J. Ryan, M. A. Angadol, J. W. Ziller and W. J. Evans, *Chem. Commun.*, 2019, **55**, 2325-2327.
- F.-S. Guo, N. Tsoureas, G.-Z. Huang, M.-L. Tong, A. Mansikkamäki and R. A. Layfield, *Angew. Chem., Int. Ed.*, 2020, **59**, 2299-2303.
- J. C. Wedal, F. Furche and W. J. Evans, *Inorg. Chem.*, 2021, **60**, 16316-16325.
- M. Keener, R. A. K. Shivaraam, T. Rajeshkumar, M. Tricoire, R. Scopelliti, I. Živković, A.-S. Chauvin, L. Maron and M. Mazzanti, *J. Am. Chem. Soc.*, 2023, **145**, 16271-16283.
- M. D. Straub, E. T. Ouellette, M. A. Boreen, R. D. Britt, K. Chakarawet, I. Douair, C. A. Gould, L. Maron, I. Del Rosal, D. Villarreal, S. G. Minasian and J. Arnold, *J. Am. Chem. Soc.*, 2021, **143**, 19748-19760.
- R. A. Keerthi Shivaraam, M. Keener, D. K. Modder, T. Rajeshkumar, I. Živković, R. Scopelliti, L. Maron and M. Mazzanti, *Angew. Chem., Int. Ed.*, 2023, **62**, e202304051.
- L. Barluzzi, S. R. Giblin, A. Mansikkamäki and R. A. Layfield, *J. Am. Chem. Soc.*, 2022, **144**, 18229-18233.
- M. Niemeyer and P. P. Power, *Inorg. Chem.*, 1996, **35**, 7264-7272.
- B. Twamley, C.-S. Hwang, N. J. Hardman and P. P. Power, *J. Organomet. Chem.*, 2000, **609**, 152-160.
- C. Stanciu, Marilyn M. Olmstead, Andrew D. Phillips, M. Stender and Philip P. Power, *Eur. J. Inorg. Chem.*, 2003, 3495-3500.
- T. Nguyen, A. Panda, M. M. Olmstead, A. F. Richards, M. Stender, M. Brynda and P. P. Power, *J. Am. Chem. Soc.*, 2005, **127**, 8545-8552.
- W. A. Merrill, T. A. Stich, M. Brynda, G. J. Yeagle, J. C. Fettinger, R. De Hont, W. M. Reiff, C. E. Schulz, R. D. Britt and P. P. Power, *J. Am. Chem. Soc.*, 2009, **131**, 12693-12702.
- C. Ni, B. Rekken, J. C. Fettinger, G. J. Long and P. P. Power, *Dalton Trans.*, 2009, 8349-8355.
- J. N. Boynton, W. A. Merrill, W. M. Reiff, J. C. Fettinger and P. P. Power, *Inorg. Chem.*, 2012, **51**, 3212-3219.
- J. N. Boynton, J.-D. Guo, F. Grandjean, J. C. Fettinger, S. Nagase, G. J. Long and P. P. Power, *Inorg. Chem.*, 2013, **52**, 14216-14223.
- J. N. Boynton, J.-D. Guo, J. C. Fettinger, C. E. Melton, S. Nagase and P. P. Power, *J. Am. Chem. Soc.*, 2013, **135**, 10720-10728.
- A. M. Bryan, W. A. Merrill, W. M. Reiff, J. C. Fettinger and P. P. Power, *Inorg. Chem.*, 2012, **51**, 3366-3373.
- B. D. Rekken, T. M. Brown, J. C. Fettinger, H. M. Tuononen and P. P. Power, *J. Am. Chem. Soc.*, 2012, **134**, 6504-6507.
- B. D. Rekken, T. M. Brown, J. C. Fettinger, F. Lips, H. M. Tuononen, R. H. Herber and P. P. Power, *J. Am. Chem. Soc.*, 2013, **135**, 10134-10148.
- M. Niemeyer, *Eur. J. Inorg. Chem.*, 2001, 1969-1981.
- A. Cofone and M. Niemeyer, *Z. Anorg. Allg. Chem.*, 2006, **632**, 1930-1932.
- P. Zhao, Q. Zhu, J. C. Fettinger and P. Power, *Inorg. Chem.*, 2018, **57**, 14044-14046.
- R. Jena, F. Benner, F. Delano, D. Holmes, J. McCracken, S. Demir and A. L. Odom, *Chem. Sci.*, 2023, **14**, 4257-4264.
- R. E. MacKenzie, T. Hajdu, J. A. Seed, G. F. S. Whitehead, R. W. Adams, N. F. Chilton, D. Collison, E. J. L. McInnes and C. A. P. Goodwin, *Chem. Sci.*, 2024, **15**, 15160-15169.
- K. Gilbert-Bass, C. R. Stennett, R. Grotjahn, J. W. Ziller, F. Furche and W. J. Evans, *Chem. Commun.*, 2024, **60**, 4601-4604.
- B. L. L. Réant, J. A. Seed, G. F. S. Whitehead and C. A. P. Goodwin, *Inorg. Chem.*, 2025, **64**, 3161-3177.
- C. D. Carmichael, N. A. Jones and P. L. Arnold, *Inorg. Chem.*, 2008, **47**, 8577-8579.
- S.-O. Hauber and M. Niemeyer, *Chem. Commun.*, 2007, 275-277.
- M. A. Lockwood, P. E. Fanwick, O. Eisenstein and I. P. Rothwell, *J. Am. Chem. Soc.*, 1996, **118**, 2762-2763.
- D. K. Modder, C. T. Palumbo, I. Douair, R. Scopelliti, L. Maron and M. Mazzanti, *Chem. Sci.*, 2021, **12**, 6153-6158.
- D. Wang, W. Ding, G. Hou, G. Zi and M. D. Walter, *Chem. Eur. J.*, 2021, **27**, 6767-6782.
- S. Wang, D. Wang, T. Li, Y. Heng, G. Hou, G. Zi and M. D. Walter, *Organometallics*, 2022, **41**, 1543-1557.
- T. W. Hayton, J. M. Boncella, B. L. Scott, P. D. Palmer, E. R. Batista and P. J. Hay, *Science*, 2005, **310**, 1941-1943.
- J. J. Kiernicki, M. G. Ferrier, J. S. Lezama Pacheco, H. S. La Pierre, B. W. Stein, M. Zeller, S. A. Kozimor and S. C. Bart, *J. Am. Chem. Soc.*, 2016, **138**, 13941-13951.
- N. C. Tomson, N. H. Anderson, A. M. Tondreau, B. L. Scott and J. M. Boncella, *Dalton Trans.*, 2019, **48**, 10865-10873.
- D. Schädle and R. Anwänder, *Chem. Soc. Rev.*, 2019, **48**, 5752-5805.
- L. Maria and J. Marçalo, *Inorganics*, 2022, **10**, 121.
- F.-S. Guo, Y.-C. Chen, M.-L. Tong, A. Mansikkamäki and R. A. Layfield, *Angew. Chem., Int. Ed.*, 2019, **58**, 10163-10167.
- J. C. Wedal, J. M. Barlow, J. W. Ziller, J. Y. Yang and W. J. Evans, *Chem. Sci.*, 2021, **12**, 8501-8511.
- W. Huang and P. L. Diaconescu, *Dalton Trans.*, 2015, **44**, 15360-15371.
- S. R. Chowdhury, C. A. P. Goodwin and B. Vlaisavljevich, *Chem. Sci.*, 2024, **15**, 1810-1819.
- L. A. Polly and T. L. Stephen, *C. R. Chim.*, 2008, **11**, 603-611.

CCDC numbers 2413501 (**1**), 2413502 (**2**), 2413599 (**3**), and 2416631 (**4**) contain the crystallographic data associated with this paper. Experimental details, computational details, and spectroscopy data are reported in the supporting information.